UC Irvine

Title

Lens-free endoscopy probe for optical coherence tomography.

Permalink

Journal

ISSN

Authors

Moon, Sucbei
Piao, Zhonglie
Kim, Chang-Seok
et al.

Publication Date

DOI

Copyright Information

Peer reviewed

Lens-free endoscopy probe for optical coherence tomography

Sucbei Moon[1,*], **Zhonglie Piao**[2], **Chang-Seok Kim**[2], and **Zhongping Chen**[2,3]

[1]Department of Physics, Kookmin University, Seoul 136-702, South Korea

[2]Department of Cogno Mechatronics Engineering, WCU Program, Pusan National University, Busan 609-735, South Korea

[3]Beckman Laser Institute, University of California, Irvine, California 92617, USA

Abstract

We present an ultrathin fiber-optic endoscopy probe for optical coherence tomography (OCT), which is made of a series of fused optical fibers instead of the conventional scheme based on an objective lens. The large-core fiber with a core diameter of 20 μm was utilized for the probe, while a single-mode fiber of core diameter 8.2 μm mainly delivered the OCT light. Those fibers were spliced with a bridge fiber of an intermediate core size. The guided light was stepwise converted to a beam of a large mode-field diameter to be radiated with a larger depth of focus. We obtained a 125 μm thick all-fiber endoscopy probe with a side-viewing capability implemented by an angled fiber end. Successful OCT imaging was demonstrated with a swept-source OCT system and showed the practical applicability of our lens-free endoscopy probe.

Advances in miniaturized endoscopy probes for optical coherence tomography (OCT) have evolved to make OCT endoscopy a useful tool for noninvasive or minimally invasive medical diagnosis [1–4]. The accessibility of the endoscopy probes to internal organs substantially depends on the size of the probing optics. Downsizing the components, such as an objective lens, has made a thin OCT endoscopy probe possible that can be as small as ~100 μm in diameter for the probe body [2]. Further size reduction seems blocked by the practical size limit of the objective lens. Note that the maximum working distance from the probe to the focus of the beam shrinks as the lens diameter decreases for a given numerical aperture. An alternative approach may be preferred for an ultrathin probe.

Fiber alone can play the role of an OCT probe without any additional optics. The side-viewing capability can also be obtained by an angled fiber end, as Sharma and Kang demonstrated with a primitive side-viewing bare-fiber OCT probe made of a conventional single-mode fiber (SMF) [3]. But it is difficult to fulfill the requirements for practical OCT imaging with the SMF alone because of the high divergence of the beam radiated by the SMF, which automatically results in a narrow depth of focus (DOF) or a small axial imaging range of OCT. In our previous investigation, we found that this limitation can be alleviated by utilizing a large-core fiber (LCF) [4], if the obstacles involved with the presence of the multiple guiding modes are avoided by proper manipulation of the high-order mode (HOM). The LCF can provide an enhanced DOF, proportional to the square of the mode-field diameter (MFD) of the probe fiber. The LCF of 20 μm core diameter was observed to lead to a four times larger DOF compared to the standard SMF. With the help of a mode-filtering scheme, the effect of the HOM was suppressed for sensitive OCT imaging. It should be noted that an SMF of, simply, a larger core and a decreased core-to-cladding index contrast

is not practical for OCT endoscopy because of the unacceptably high bend sensitivity, which restricts the flexibility of the fiber [4,5].

In this Letter, we present an alternative OCT endoscopy approach to conventional lens-based optics. Our OCT endoscopy probe consists of a series of fused optical fibers that moderate the guided light for an enhanced DOF. The effect of the HOM was avoided by optimized fiber parameters without additional mode filtering. Hence, the diameter of the probe is limited only by the size of the fiber core and the thickness of the necessary cladding layer in our probe. The structural simplicity of our probe is attractive in terms of the fabrication cost, performance predictability, and reliability, even though the achievable axial imaging range decreases to half of the length that the lens-based probe can provide.

The structure of our bare-fiber OCT probe is illustrated by Fig. 1. It is an optical fiber with an angled surface at the end. The light guided by the fiber core was reflected by the end surface to make a nearly perpendicular beam running out of the fiber. The actual angle of the end surface was made to be $\phi = 41°$ with respect to the fiber axis so that the beam reflected by the total internal reflection deviated from the perpendicular plane by $8°$. This could prevent the reflection at the cladding surface from producing excessive signals backreflected to the core.

Three types of fiber were used, including the standard SMF (SMF-28e, Corning Inc.) that mainly delivered the OCT light from the source to the probe. At the end of the probe, a short section of LCF (Liekki Passive-20/125, nLight Corp.) was utilized for the large MFD. Another short section of bridge fiber (BF) of an intermediate core size (Liekki Passive-12/125) was placed between them so that the core diameter increased stepwise, as it was 8.2 μm in the SMF, 12.5 μm in the BF, and 20 μm in the LCF. All of the fibers were spliced by a conventional fusion splicer with ease. After the fused fiber was prepared, the angled end surface was made by polishing the fiber end. Those fibers used in our probe were all 125 μm thick in diameter. Each section of the LCF and BF was 10 mm long, enough to prevent the guided modes from being interfered with the fields leaked by the prior spliced points. In endoscopy imaging, our probe was inserted into a thin capillary tubing (TSP150375, Molex Inc.) for protection. This protective capillary was a silica tube with 20 μm thick polyimide coating on the outside. Its inner and outer diameters were 150 and 360 μm, respectively.

The LCF section used in our probe was of the same kind as the LCF used in our previous research. The Rayleigh range of the LCF was 0.2 mm due to the large core size, which resulted in an MFD of ~20 μm for the full width at $1/e^2$ intensity measured at a wavelength of $\lambda = 1.3$ μm. More information on the LCF is available in [4]. Because this fiber supports two or three linearly polarized (LP) modes, control of the HOM's effect is a crucial part of our probe. A spurious response as a result of mode-dependent group delays would be produced in the OCT A-line, which can significantly degrade the sensitivity and the dynamic range of the imaging system. The chance of HOM excitation could be reduced by the minimized fiber misalignments in the fusion splicing step. But a nonnegligible portion of power must have been inevitably coupled to the HOM of the LCF.

The spurious OCT signal caused by the HOM appears overlaid on the main OCT signal carried by the fundamental LP_{01} mode. This is delayed by the characteristic group velocity of the HOM. For an optical fiber of length L, core refractive index n, and core-to-cladding index contrast Δ, the relative group delay with respect to that of the LP_{01} mode, δt, can be estimated by

$$\delta t = \frac{\delta N \cdot L}{c} = \frac{\alpha n \Delta \cdot L}{c} \quad (1)$$

as a rough approximation, where δN, c, and α are the group-index difference, the speed of light, and the normalized group delay, respectively. The value of α is within a range of ± 1.0 for a usual step-index fiber [6]. The LCF used in our probe has $n = 1.45$ and $\Delta = 0.16\%$, so that the relative group delay that every meter of LCF can produce is 7.7 ps at most. This corresponds to a spatial delay of 2.3 mm in free space. But for a short fiber, e.g., with $L = 10$ mm, the spurious signal, if any, must be located close to the main one with a small offset of < 23 μm in an OCT A-line. Considering that the HOM power is usually much lower than that of LP_{01}, this spurious signal could be buried by the sidelobes of the main signal. This is surely true for that of LP_{11} mode, where the relative group delay had been experimentally measured to be 2.6 μm for $L = 10$ mm [4]. The amount of the delay is small enough, just comparable to the axial resolution of a typical OCT system. If the mode power of LP_{11} were lower than 10 dB, its signal would not make a noticeable contribution.

The use of the intermediate BF may look unnecessary at first sight. But it reduces the insertion loss caused by the MFD mismatch between the SMF and the LCF as well as the chance of HOM excitation. The splicing loss of the LP_{01} mode was carefully evaluated using a fiber-coil mode filter at $\lambda = 1.3$ μm. First, the SMF was spliced directly to the LCF for comparison while keeping a section of the LCF coiled at a curvature radius of 27 mm. This coiled section suppressed the HOM by more than 30 dB; so the loss measurement was done exclusively for LP_{01} [4]. The transmitted power from the SMF to the LCF via the mode filter was measured to be 1.9 dB lower than the input power because of the SMF–LCF splicing loss for LP_{01}. In the same manner the insertion loss of the SMF–BF–LCF splices in series was measured. It was 1.0 dB, or a percentage loss of 21%. The reduced loss could be explained by the stepwise increase of the MFD in part as well as enhanced diffusion of the core dopants at the two interfaces that might occur during the fusion splicing. The abrupt change of the fiber core could be softened in those ways. A similar effect can be obtained by using a tapered fiber or thermally expanded core fiber [5,7]. Using a BF is attractive in terms of fabrication ease. Note that the decreased loss also suggests that the power coupled to the HOM was low, surely below 1/5 of the input power or probably only a few percent, so that the HOM hardly has a visible effect in the OCT image if the delay is small enough.

The axial imaging range of our probe was quantitatively evaluated by measuring the beam width as a function of the distance from the fiber core, D, at $\lambda = 1.3$ μm. A microscope equipped with an IR camera captured the shape of the beam exiting the probe. The three graphs of Fig. 2 show the change of the beam widths measured in FWHM for the bare probe alone [(Fig. 2 (a)], the probe in the capillary tube laid in the air [(Fig. 2 (b)], and the probe in the capillary immersed in the index-matching gel with a glass cover [(Fig. 2 (c)]. The beam width was evaluated on two axes: one along the perpendicular direction (–■–), and the other one in parallel to the fiber axis (··▲··). The vertical dashed line in each plot represents the position of the boundary between the glass and the surrounding medium. The horizontal axis of Fig. 2(c) was rescaled by multiplying the refractive index of the index-matching gel, $n = 1.45$. Figure 2 suggests that our probe can provide an effective axial imaging range of ~0.5 mm in tissue ($n \approx 1.4$), within which the transverse resolution varied by as much as a factor of two or smaller. For the case of Fig. 2 (c), the lateral resolution expected by the FWHM beam width ranged from 13 to 26 μm in the first 0.65 mm after the capillary.

Figure 2 (a) also shows that the beam divergence in the perpendicular axis was affected by the curvature of the fiber's or capillary's boundary surface; so they might act as cylindrical lenses [2]. This effect was not observed for the beam width in the parallel axis. In Fig. 2 (c)

with the case of the index-matched surrounding, the cylindrical lens effect was nearly neutralized with little astigmatism. Meanwhile, for the dry-capillary case in Fig. 2 (b), the curvature of the capillary effectively reduced the beam divergence in the perpendicular axis. For an aqueous endoscopic specimen such as a blood vessel, the refractive index of the surrounding media would range from 1.3 to 1.4. The beam divergence, then, would appear somewhere between those two curves of Figs. 2(b) and 2(c). It is expected that the intrinsic lens effect of the capillary may help increase the DOF slightly if properly designed with optimized parameters.

Finally, our probe was tested for OCT imaging with a swept-source OCT system that operated at an A-line rate of 50 kHz with a full spectral bandwidth of 100 nm centered at 1311 nm. The power irradiated at the sample through our OCT probe was 4.7 mW. Human finger tip and palm were used as imaging samples because of their popularity as test OCT images. Figure 3 (a) shows the OCT image of a human finger tip acquired by a push–pull scan of the probe performed inside the protective capillary. Figure 3 (b) shows the image of human palm, which was folded around our probe, acquired by rotating the probe in a circumferential scan mode. Water was applied to the sample for index matching. The acquisition time spent for each image was 100 ms for Fig. 3 (a) and 18.7 ms for Fig. 3 (b). The result of the OCT imaging well matched the performance predicted by the data of Fig. 2. Our probe provided good imaging quality for near regions within a half millimeter, while far regions were blurred by the degraded transverse resolution, which was roughly proportional to the distance from the probe. On the other hand, no significant degradation was found in the axial point-spread function except for minor artifacts. These results verify that our OCT probe took advantage of the increased DOF without a penalty caused by the multi-mode guidance.

In conclusion, we successfully demonstrated a lens-free OCT endoscopy probe in a very simple structure without significant degradation of imaging quality. An ultrathin endoscopy probe was fabricated by simply splicing and polishing fibers instead of using an optical lens. By tailoring the waveguide with various fibers, our probe converted the beam characteristic for an improved DOF and a minimized effect of the HOM for practical OCT endoscopy. The experimental result demonstrated that our probe, in spite of its simplicity, can provide good OCT imaging performance. Our scheme was found to be particularly attractive in terms of fabrication and reliability. It does not require fine alignments of optical components except for those of the well-established fusion splicing process, which makes it particularly attractive to produce and fabricate a truly disposable low-cost endoscopy probe.

Acknowledgments

References

1. Yaqoob Z, Wu J, McDowell EJ, Heng X, Yang C. J. Biomed. Opt. 2006; 11:063001. [PubMed: 17212523]

2. Lorenser D, Yang X, Kirk RW, Quirk BC, McLaughlin RA, Sampson DD. Opt. Lett. 2011; 36:3894. [PubMed: 21964133]

3. Sharma U, Kang JU. Rev. Sci. Instrum. 2007; 78:113102. [PubMed: 18052460]

4. Moon S, Chen Z. Appl. Opt. 2012; 51:8262. [PubMed: 23207399]

5. Moon S, Liu G, Chen Z. Opt. Lett. 2011; 36:3362. [PubMed: 21886211]

6. Okamoto K. Fundamentals of Optical Waveguides (Academic. 2000:78–83.

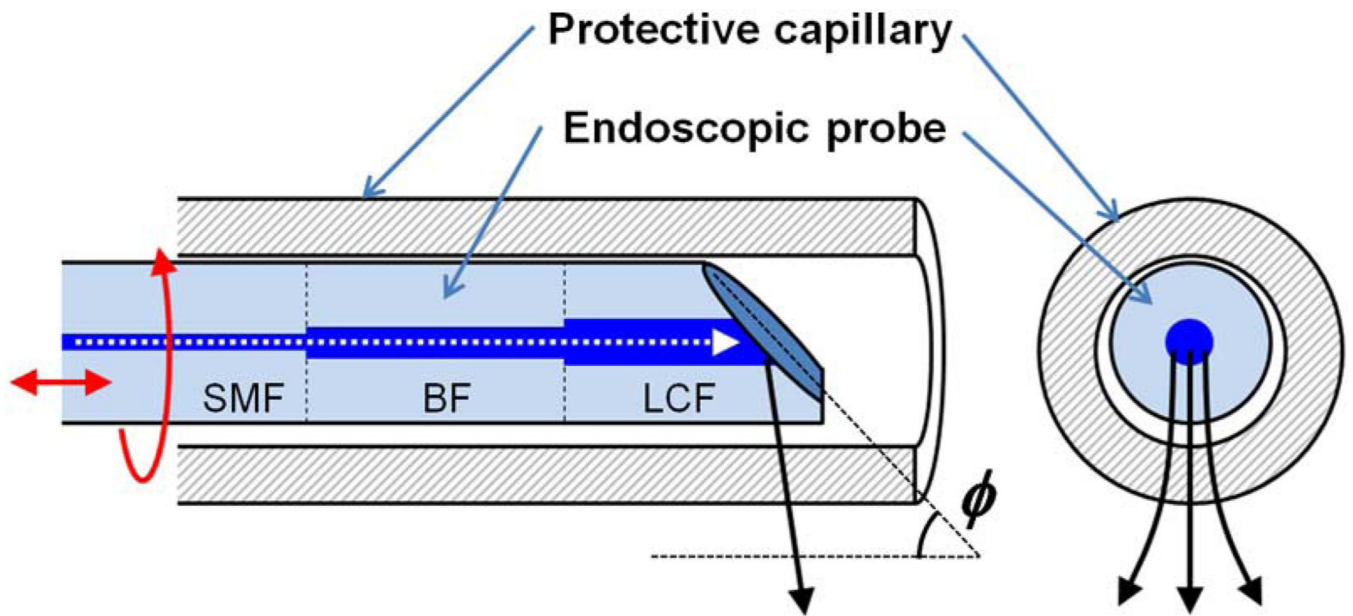7. Kim K-R, Oh K. Appl. Opt. 2003; 42:6261. [PubMed: 14649267]

Fig. 1.
Schematic of our bare-fiber OCT endoscopy probe in a protective capillary tube.
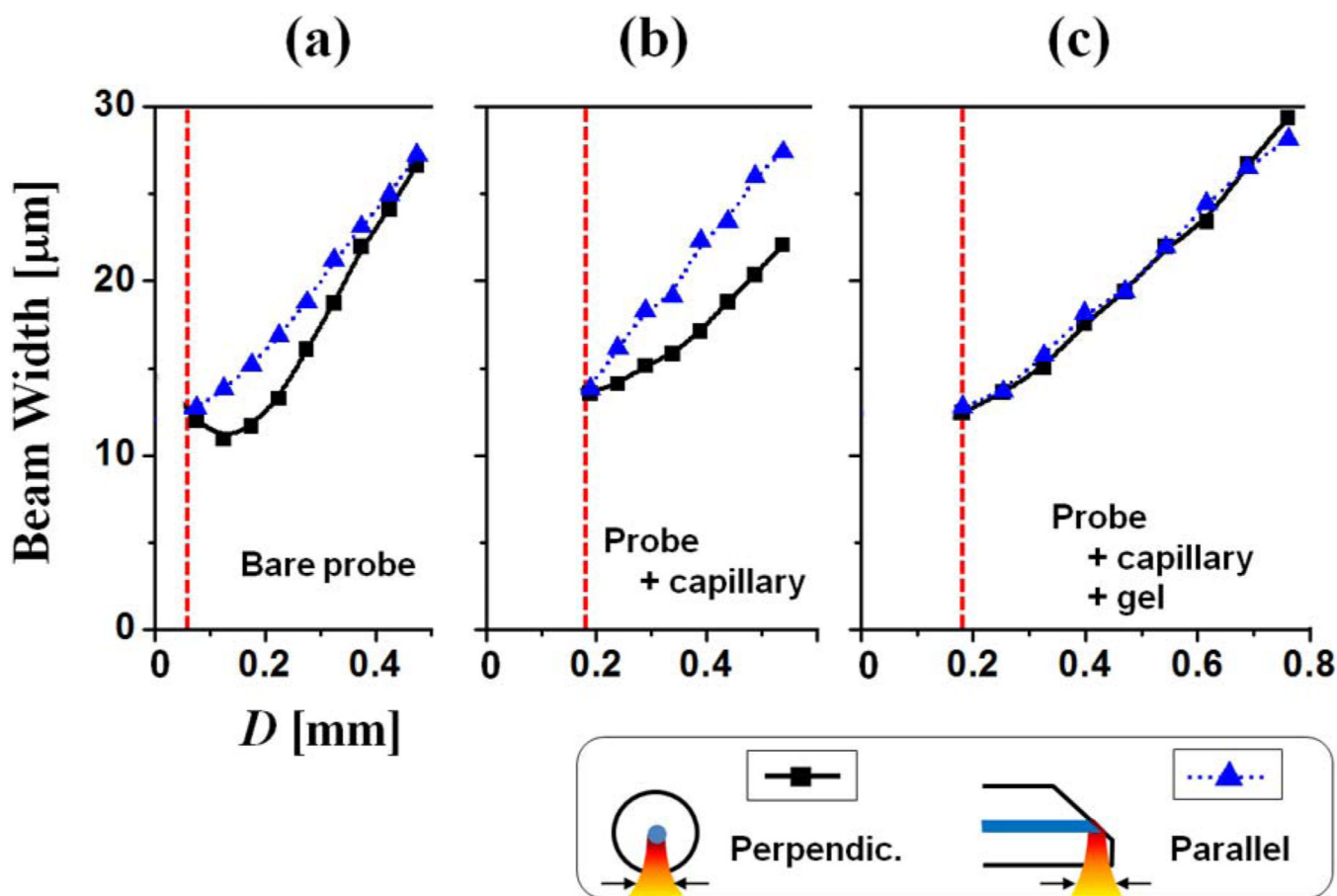
Fig. 2.
Change of the beam widths measured in the perpendicular and parallel axes for (a) the bare probe alone, (b) the probe in the capillary tube laid in the air, and (c) the probe in the capillary immerged in the index-matching gel.
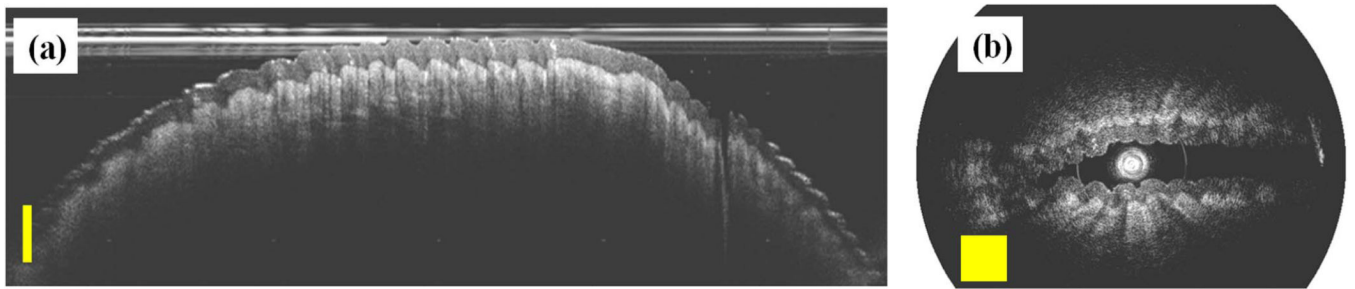
Fig. 3.
OCT images of human finger tip and palm acquired by (a) a push–pull scan and (b) a circumferential scan. The length of the inset rectangle or square corresponds to 1 mm in air.